

# A Wide Frequency Range Surface Integral Formulation for 3-D Inductance and Resistance Extraction

J. Wang\*, J. Tausch\*\* and J. White\*

\* Department of Electrical Engineering and Computer Science, M.I.T. Cambridge, MA. 02139

\*\* Southern Methodist University, tausch@golem.math.smu.edu

## ABSTRACT

A new surface integral formulation and discretization approach for computing the magnetoquasistatic impedance of general conductors is described. The key advantage of the formulation is that it correctly predicts the resistance and inductance over the entire frequency. In addition, since the formulation is directly derived from Maxwell's equations under the MQS assumption, it does not require a-priori information about skin depth nor does it include assumptions about proximity effects. Computational results for a ring and a wire are presented to verify the formulation.

**Keywords:** Electromagnetics, Impedance extraction, Surface integral equation, PEEC, FastHenry,

## 1 Introduction

Many approaches to impedance extraction exploit the close connection between circuit analysis, which relies primarily on current conservation, and the electromagnetic analysis, in which there are field quantities such as potentials and current densities. In such formulations, current distributions are represented directly by discretizing the volume of the conductor [1], but this volume discretization makes it difficult to analyze complicated geometries over a wide range of frequencies. In complicated geometries it is cumbersome to generate the volume meshes in the conductors, and in addition, the mesh must be adapted as the frequency rises to model the skin effect. In order to address this problem, very effective techniques based on surface impedances have been developed [2], [3], but these approaches make some assumptions about proximity effects.

In this paper we describe a surface integral formulation and discretization approach to computing the magnetoquasistatic impedance of general conductors. The key advantage of this new formulation is that it correctly predicts the frequency dependent resistance and inductance using a single formulation. In addition, since the formulation is directly derived from Maxwell's equations under the MQS assumption, it does not require a-priori information about surface impedances nor does it include assumptions about proximity effects. In the next sec-

tion, the integral formulation and discretization for thin conductors is derived. In section 3, we present some preliminary results for a ring and a single wire example and compare to the publicly available FastHenry program. Finally, conclusions are given in Section 4.

## 2 Surface formulation

There is a similarity between our surface formulation and the nodal analysis approach to computing the impedance of a complicated circuit. To compute impedances using nodal analysis, two basic relationships are necessary. First, there should be a constitutive relationship between the potential drop and the current; secondly, there should be current conservation. The surface formulation below has corresponding relationships, but the approach also requires a relation between the surface electric field and its normal derivative. This second equation is necessary because it ensures that the surface quantity is a complete representation of the volume.

### 2.1 Equation System

There are two integral and one differential equation our surface formulation. They are described below.

#### 2.1.1 First dyadic surface integral equation

Assume a conductor has surface  $S$  and volume  $V$ . Under the magnetoquasistatics(MQS) assumption,  $E$  in time-harmonics is governed by the dyadic Helmholtz equation over the whole volume of  $V$ :

$$\nabla^2 \bar{E} - i\omega\mu\sigma \bar{E} = 0 \quad (1)$$

Applying Green's Theorem to 1 in the interior of  $S$ , a dyadic surface integral equation can be derived:

$$\int_S G_1(x, y) \frac{\partial \bar{E}(y)}{\partial n_y} dy - \int_S \frac{\partial G_1(x, y)}{\partial n_y} \bar{E}(y) dy = \bar{E}(x) \quad (2)$$

where

$$G_1(x, y) = \frac{e^{ik_1|x-y|}}{4\pi|x-y|}, \quad k_1 = \text{sqrt}(-i\omega\mu\sigma)$$

$x$  and  $y$  are on  $S$ , and the singularity in  $\int_S \frac{\partial G_1(x, y)}{\partial n_y} \bar{E}(y) dy$  is not removed.

### 2.1.2 Second dyadic surface integral equation

Another way of writing the dyadic Helmholtz equation for  $E$  in time-harmonics under magnetoquasistatics is:

$$\nabla^2 \bar{E} = i\omega\mu\bar{J} \quad (3)$$

Applying Green's Theorem to 3 in the interior of  $S$  results in an integral equation of the form:

$$\begin{aligned} \int_S G_0(x, y) \frac{\partial \bar{E}(y)}{\partial n_y} dy - \int_S \frac{\partial G_0(x, y)}{\partial n_y} \bar{E}(y) dy \\ = \bar{E}(x) + i\omega \int_V \mu G_0(x, y) \bar{J}(y) dy \end{aligned}$$

where

$$G_0(x, y) = \frac{1}{4\pi|x-y|}$$

With  $-\nabla\psi = E + i\omega A$  and  $\bar{A}(x) = \int_V \mu G_0(x, y) \bar{J}(y) dy$ , the integral equation above can be written as:

$$\begin{aligned} \int_S G_0(x, y) \frac{\partial \bar{E}(y)}{\partial n_y} dy \\ - \int_S \frac{\partial G_0(x, y)}{\partial n_y} \bar{E}(y) dy + \nabla\psi(x) = 0 \quad (4) \end{aligned}$$

Again, the singularity in the integration is not removed.

### 2.1.3 Current conservation

The equations derived above are only two equations for three variables  $E$ ,  $\frac{\partial E}{\partial n}$  and  $\psi$ , and another equation is necessary. There are two approaches that might yield the equation needed. One is to enforce  $\nabla^2\psi = 0$ , another is to enforce current conservation ( $\nabla \bullet E = 0$ ). For a closed loop, both approaches are equivalent, but for an open loop,  $\nabla^2\psi = 0$  is no longer true, while  $\nabla \bullet E = 0$  still holds. Therefore, current conservation is enforced for all cases.

### 2.1.4 Boundary conditions

Two boundary conditions are used for the conductor contacts. The potential at the contacts is given, and it is assumed that there is no tangential current flow at the contacts. As the electric field is divergence free,  $\frac{\partial E_n}{\partial n}$  must be zero at the contacts.

## 2.2 Thin Conductor Analysis

To investigate the above formulation for thin structures like the ring in Figure 1, the current is assumed to follow the path of the conductor.

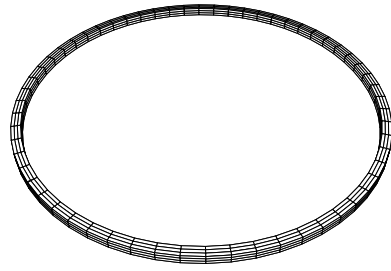


Figure 1: A discretized ring

### 2.2.1 Discretization

To discretize the problem, the surface is decomposed into flat panels. The panels at the contacts of the conductor where potential is applied are called contact panels, while the other panels are called non-contact panels. On each panel,  $E$  is assumed to be nonzero only in the direction of the length of the conductor, which is denoted by a unit vector  $f$ . For each panel, there are two unknowns  $E_f = \bar{E} \bullet f$  and  $\frac{\partial E_f}{\partial n} = \frac{\partial \bar{E}}{\partial n} \bullet f$ .

To represent  $\nabla_f\psi$  of non-contact panels using a finite difference scheme, potential nodes are put at the midpoint of the edges of non-contact panels orthogonal to the direction of current, see Figure 2.

### 2.2.2 Linear system

Using a constant-strength collocation scheme, the two surface integral equations 2 and 4 take the form:

$$P_{1f} \frac{\partial E_f}{\partial n} - (D_{1f} + \frac{1}{2}I)E_f = 0 \quad (5)$$

$$P_{0f} \frac{\partial E_f}{\partial n} - D_{0f}E_f + \nabla_f\psi = 0 \quad (6)$$

where

$$P_{1f}(i, j) = (f_i \bullet f_j) \int_{panel_j} G_1(x_i, y) dy$$

$$D_{1f}(i, j) = (f_i \bullet f_j) \int_{panel_j} \frac{\partial G_1}{\partial n_y}(x_i, y) dy$$

$$P_{0f}(i, j) = (f_i \bullet f_j) \int_{panel_j} G_0(x_i, y) dy$$

$$D_{0f}(i, j) = (f_i \bullet f_j) \int_{panel_j} \frac{\partial G_0}{\partial n_y}(x_i, y) dy$$

where  $I$  is identity matrix and  $x_i$  is the center of the  $i$ th panel.

To form the linear system of equations, equation 5 is applied to all panels. Equation 6, however, is only applied to non-contact panels because for the contact panels,  $\frac{\partial E_f}{\partial n} = 0$ . This boundary condition results from the observation that the electric field is always divergence free.

The gradient of the potential, needed in 6, is derived from node potentials. As shown in Figure 2, two potential nodes  $N_1$  and  $N_2$  are placed at the midpoint of the edges of panel 2 orthogonal to the direction of current, then

$$\nabla_f \psi \approx (\psi(N_2) - \psi(N_1))/L$$

where  $L$  is the distance between the two potential nodes.

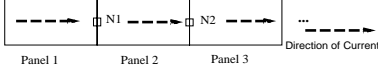


Figure 2: The position of nodes with unknown potential

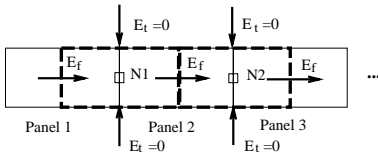


Figure 3: Current conservation in 1-D form

In order to enforce the current conservation equation, consider the diagram shown in Figure 3. The two areas enclosed by the dashed thick lines are the top of the thin boxes around  $N_1$  and  $N_2$ , the nodes with unknown potential. The normal current is zero under the MQS assumption, and the tangential current orthogonal to the wire direction, that is orthogonal to  $f$ , is also zero under the thin conductor assumption. Therefore,  $E_f$  has to be the same through the current path,

$$E_f(x_1) = E_f(x_2) = E_f(x_3). \quad (7)$$

For every node on the side, there is one surface current conservation equation. There are exactly the same number of surface current conservation equation as the number of nodes with unknown potential.

The three set of equations, 5, 6 and 7, and the boundary condition for  $\frac{\partial E_f}{\partial n}$  at the contacts, results in a nonsingular system for determining the node potentials and the panel currents.

### 2.2.3 Current computation

Once the linear system is solved, the current flowing into the conductor can be computed. At low frequency, current can be computed by summing up the current flowing into the contact panels. At high frequency, a more accurate approach is to use  $\int_l \vec{H}(x)dx$  instead, where  $l$  is a closed line encircling the cross-section of the conductor. Using relationship between  $E$  and  $H$ , the current is actually

$\int_l \frac{\partial E_f(x)}{\partial n_x} dx / (i\omega\mu)$ . When the skin depth is about one fourth of that of the diameter of the cross section, the current is computed using the magnetic approach. Finally, the impedance is the reciprocal of the current due to a unit potential source, and the resistance and inductance are computed from the impedance.

## 3 Numerical experiments

To test this new surface formulation for long thin structure, we use the ring in Figure 1 and compared the result of surface formulation to both analytical result at low frequency and results from the FastHenry simulation program. FastHenry combines multipole acceleration with a PEEC-like volume method [6]. As shown in Figure 4, both simulation methods match the analytic inductance for the low frequency range (The low frequency analytic inductance is 0.04889 nH, computed with formula from [8]), and both show the drop in inductance due to the skin effect at high frequency. However, the convergence of inductance is more frequency dependent for surface method than for FastHenry. As can be seen from the curves for 272 panels and 848 panels in Figure 4, the convergence is slowest around 10 GHz, when skin depth is close to the diameter of the cross section.

When examining the resistance, shown in (Figure 5), the two methods behave very differently. The surface formulation captures the frequency dependence of the resistance, due to the skin effect, without changing the discretization (848 surface panels were used). For FastHenry, however, the resistance stops increasing at a frequency that is discretization dependent. Figure 5 shows the higher frequency resistance computed with FastHenry change dramatically for 1440, 3840, and 15360 filaments.

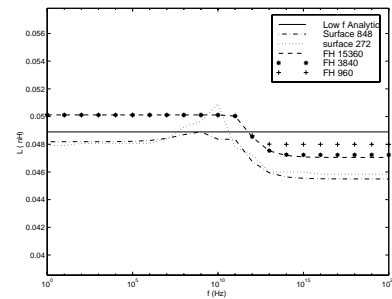


Figure 4: Inductance for the ring example

Another example used is a straight conductor wire which is 8  $\mu\text{m}$  long, 1  $\mu\text{m}$  wide and 1  $\mu\text{m}$  thick. The surface formulation is using 160 panels over the whole frequency range, while FastHenry is using 128, 512 and 2048 filaments. The observation is similar to the ring example. As shown in Fig-

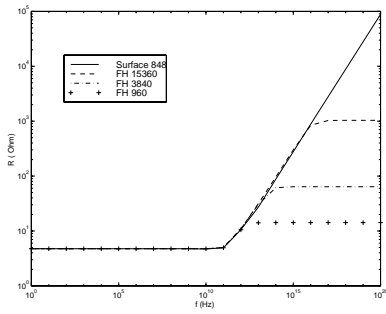


Figure 5: Resistance for the ring example

ure 6, two method shows similar inductance over the whole range, and both capture the inductance drop due to the skin effect; For resistance result as shown in Figure 7, surface formulation still captures the frequency dependency without changing the discretization while the high frequency resistance computed with FastHenry changes dramatically for 128, 512 and 2048 filaments.

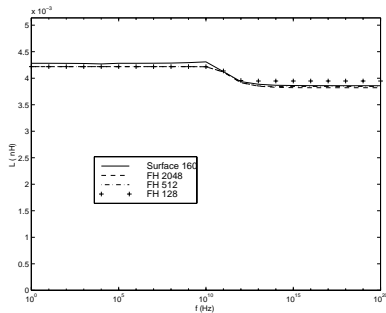


Figure 6: Inductance for the wire example

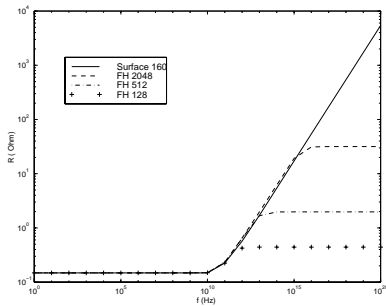


Figure 7: Resistance for the wire example

## 4 conclusions and acknowledgements

In this paper a new surface integral formulation and discretization approach for computing the magnetoquasistatic impedance of general conductors was described. The key advantage of the formulation is that it correctly predicts impedances over the entire frequency range. Computational results for a ring and a wire were presented to verify that

the formulation can accurately predict the frequency dependence of resistance and inductance over the entire frequency range without modifying the discretization.

The authors would like to thank Matt Kamon his help with the FastHenry code. This work was supported by the DARPA composite CAD program, the DARPA muri program, and grants from the Semiconductor Research Corporation.

## REFERENCES

- [1] P. A. Brennan, N. Raver, and A. Ruehli, "Three dimensional inductance computations with partial element equivalent circuits," *IBM Journal of Res. and Develop.*, vol. 23, pp. 661–668, November 1979.
- [2] E. Tuncer, Beom-Taek Lee, and D. P. Neikirk, "Interconnect Series Impedance Determination Using a Surface Ribbon Method" *IEEE 3rd Topical Meeting on Electrical Performance of Electronic Packaging*, Monterey, CA, Nov. 2-4, 1994, pp. 250-252.
- [3] R.B. Wu and J.C. Yang, "Boundary integral equation formulation of skin effect problem in multiconductor transmission lines" *IEEE Trans. Magnetics*, vol. Mag-25, pp.3013-3015, July 1989.
- [4] A.R. Djordjevic, T.K. Sarkar, and S.M. Rao, "Analysis of finite conductivity cylindrical conductors excited by axially-independent TM electromagnetic field" *IEEE Trans. Microwave Theory Tech.*, vol.MTT-33, pp.960-966, Oct.1985.
- [5] M.J. Tsuk and J.A.Kong, "A Hybrid Method for the calculation of the resistance and inductance of transmission lines with arbitrary cross sections" *Microelectronic System Interconnections*, pp65-pp74.
- [6] M. Kamon M.J. Tsuk and J.K. White, "FASTHENRY: A multipole accelerated 3-D Inductance Extraction Program", *IEEE Trans. MTT*, vol.42., No.9, pp1750-pp1758, Sep.1994.
- [7] H.Heeb and Albert Ruehli, "Three-dimensional interconnect analysis using Partial Element Equivalent Circuits", *IEEE Trans. on Circuits and Systems*, vol.39, No.11, Nov. 1992.
- [8] Grover, Frederick Warren, "Inductance calculations, working formulas and tables", New York, 1946.